Advanced Functional Materials

ADVANCED FUNCTIONAL MATERIALS
www.afm-journal.de

RESEARCH ARTICLE

Harnessing Oscillatory Dynamics for Reprogrammable Mechanical Functionality

Sophie Monnery[1] | Giada Risso[2] | Loucas Plado Costante[2] | Arnaud Lazarus[1,3] | Katia Bertoldi[2]

[1]Institut Jean le Rond d'Alembert, CNRS UMR7190, Sorbonne Université, Paris, France | [2]J.A. Paulson School of Engineering and Applied Sciences, Harvard University, Cambridge, USA | [3]Massachusetts Institute of Technology, Department of Mathematics, Cambridge, USA

Correspondence: Arnaud Lazarus (arnaud.lazarus@upmc.fr) | Katia Bertoldi (bertoldi@seas.harvard.edu)

Received: 7 January 2026 | **Revised:** 20 March 2026 | **Accepted:** 24 March 2026

ABSTRACT

Achieving true mechanical reprogrammability — where structural functions can be dynamically defined, modified, and accessed on demand — requires the ability to arbitrarily set and alter the states of arrays of mechanical bits. Here, we introduce a new approach that accomplishes exactly this by exploiting asynchronous symmetry breaking in oscillator arrays driven by a single global actuator. Using an array of pendula as an experimental model, we show that intrinsic frequency separation enables arbitrary information writing and even makes possible the realization of a mechanical piano. Because the system is controlled exclusively through the timing of a global actuation signal, this strategy offers a scalable and efficient route toward reprogrammable matter, with applicability across elastic structures, chemical oscillators, and electronic circuits.

1 | Introduction

Structures are usually designed to perform fixed functions determined by their geometry and materials, which remain unchanged even as environmental conditions or performance requirements shift. To overcome this rigidity, researchers have introduced responsiveness directly into structures, for example through smart materials that alter their properties under external stimuli [1–3] or jamming-based mechanisms [4–6]. Large deformations and instabilities have also been harnessed to realize tunable or reconfigurable responses [7–11]. Yet these approaches fall short of true mechanical reprogrammability, where structural functions can be dynamically defined, modified, and accessed on demand, akin to rewriting data on a hard drive.

To address this challenge, recent efforts have focused on building blocks that act as mechanical analogs of digital bits [12]. Bistable units are particularly attractive because their two stable states naturally replicate binary logic [13]. Programming arrays of such units has been pursued through two main strategies: individually addressing each bit [14], or exploiting interactions between neighboring units to reach desired configurations under global inputs [15–17]. The first offers full control but requires complex actuation schemes, while the second reduces actuation demands but often involves intricate loading sequences and nontrivial coupling design. To overcome these limitations, a dynamic control approach was recently introduced that enables arbitrary state transitions through global rotational driving cycles [18].

Here, we introduce an alternative approach for arbitrarily defining and modifying the state of arrays of mechanical bits, inspired by recent advances in oscillating–diverging systems [19–21]. We investigate arrays of pendula whose boundary conditions break symmetry, effectively turning each into a mechanical bit. When the actuation window is short relative to the natural oscillation timescales, the state of each pendulum can be programmed solely through the timing of a single global boundary condition. This enables rapid reprogramming, arbitrary information writing, and even the construction of a "mechanical piano" capable of producing user-defined sequences of notes and chords within only a few oscillation periods. In contrast to the rotating platform, which requires precise control of both angular velocity and acceleration

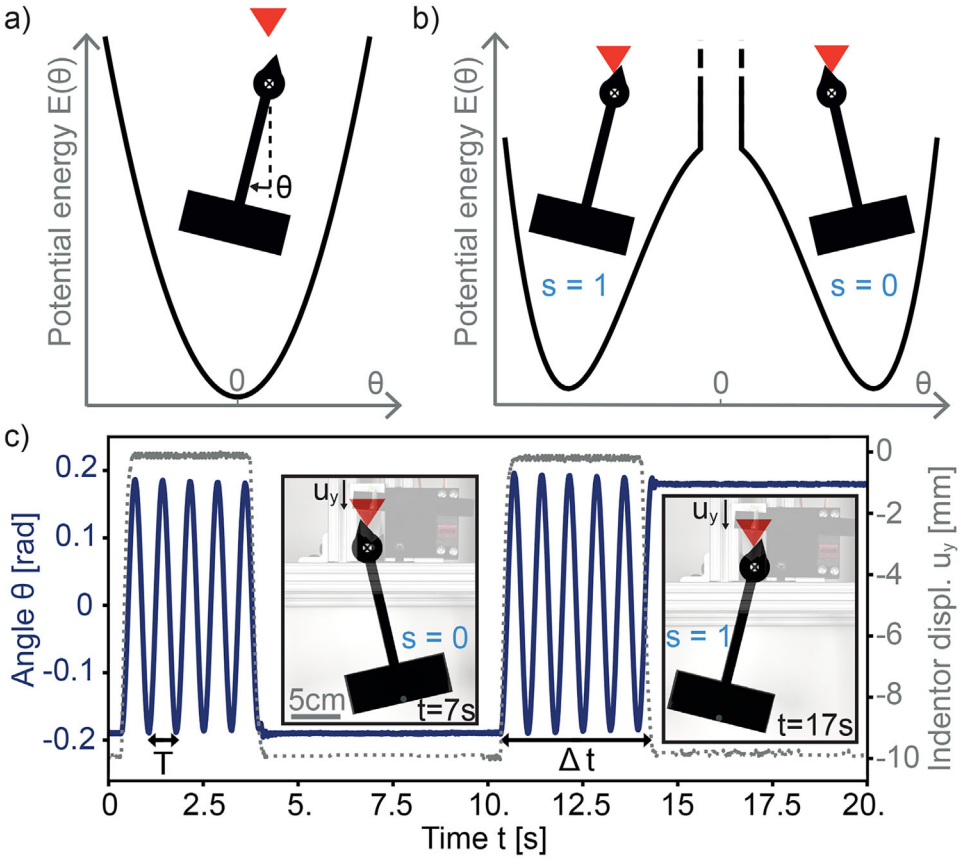

FIGURE 1 | Mechanical bit. (a) Schematic of the globally convex energy landscape of a freely oscillating pendulum. (b) Schematic of the energy landscape when the indenter is lowered, breaking the symmetry of the system. (c) Experimental time evolution of the pendulum angular motion (left axis) together with the indenter displacement u_y (right axis). The pendulum has a natural period $T = 0.72$ s. Insets show snapshots of the pendulum locked in state $s = 0$ at $t = 7$ s and in state $s = 1$ at $t = 17$ s.

to set the states of bistable bits [18], our system is driven by a single parameter (time) and allows straightforward readout through direct physical interaction with the environment. Because it integrates seamlessly with diverse functionalities, this strategy establishes a scalable framework for dynamic, efficient, and reprogrammable mechanical systems.

2 | Our Hybrid Mechanical Bit

Mechanical bits are typically non-volatile, implemented using bistable structures with a double-well energy landscape in which each stable configuration represents a digital state, either state 0 or state 1 [13, 14]. A key advantage of this approach is that the states are inherently robust and require no external energy to be maintained. However, switching between states requires an external energy input to drive the transition. In contrast, monostable structures exhibit a globally convex energy landscape with a single stable equilibrium configuration (Figure 1a). While they are not inherently suited for storing states, they can still be used for mechanical computing by harnessing their predictable harmonic oscillations and associating logical states with the direction of motion [12]. However, due to damping, these oscillations decay over time and persist only when energy is continuously supplied through external excitation, thereby mimicking the behavior of volatile memory [22]. A promising pathway toward mechanical reprogrammable systems is to develop a hybrid system that can switch between monostable and bistable energy landscapes through a single control parameter. In this framework, the bistable (double-well) phase serves as a non-volatile regime that stores mechanical information without continuous energy input, while the monostable (single-well) phase introduces volatility and allows the system to be reprogrammed.

Here, we present a proof-of-concept for a hybrid mechanical bit that operates by kinematically breaking the symmetry of an oscillating pendulum. Unlike conventional bistable structures, where the geometry itself gives rise to two energy minima [23], the double-well energy landscape in our system is generated by a vertically actuated indenter, whose motion is driven by two servomotors. When the indenter is raised, the pendulum oscillates freely and exhibits a single energy minimum when aligned vertically (i.e., at $\theta = 0$ - Figure 1a). Lowering the indenter reshapes the energy landscape into two potential wells separated by an effectively infinite energy barrier, thereby locking the pendulum into one of the wells, each corresponding to a distinct state (Figure 1b). The well in which the pendulum settles is determined by its angular displacement θ at the moment of actuation. If the indenter is lowered while θ is positive, the pendulum is captured to the left of the vertical axis, which we define as state $s = 1$ (Figure 1c). If instead it is lowered when θ is negative, the pendulum settles to the right, corresponding to

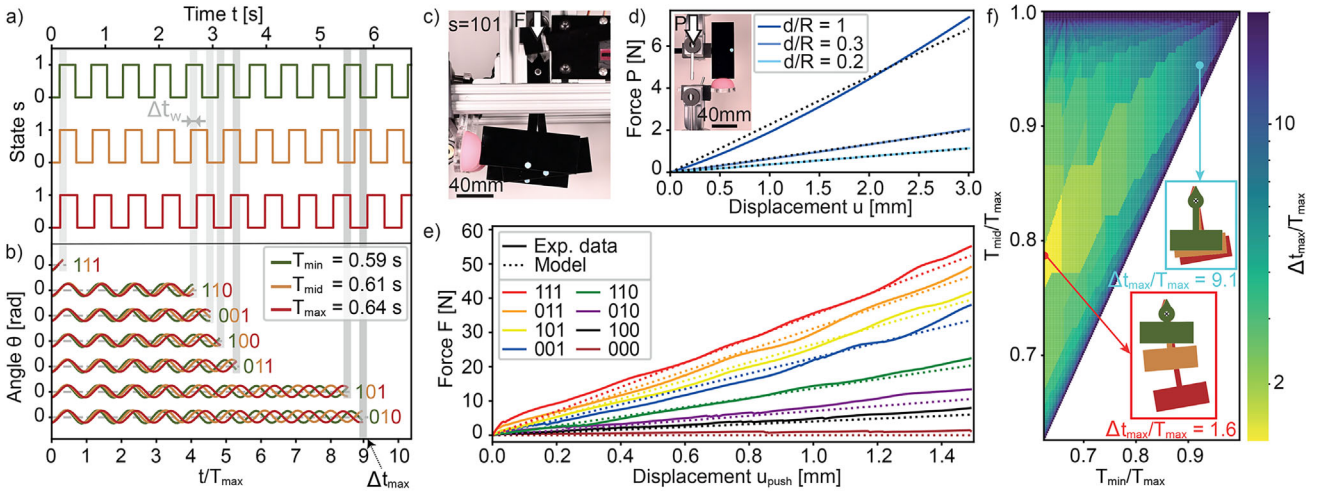

FIGURE 2 | State programming via desynchronization. (a) Temporal evolution of $s(t)$ for three pendula with $T_{\min} = 0.59$ s, $T_{\mathrm{mid}} = 0.61$ s, and $T_{\max} = 0.64$ s. Gray windows indicate intervals $\Delta t_w = 0.1$ s during which all three pendula occupy the desired state. (b) Experimental temporal evolution of the angular positions $\theta(t)$ of the three pendula. (c) Experimental setup of the reprogrammable linear spring. The system is shown in state 101 with three elastomeric spheres positioned on the left side of each pendulum. (d) Experimental force–displacement curves (continuous lines) for three hemispherical shells with thickness-to-radius ratio $d/R = 1$, 0.3, and 0.2 under pendulum indentation. Curves are obtained by taking the mean of three tests. Dashed lines indicate linear fits. (e) Experimental force–displacement curves obtained by further lowering the indenter with the system programmed in all eight states (continuous lines). Predictions from the summed responses of the indented shells are shown as dotted lines. (f) Numerical prediction of $\Delta t_{\max} = \max(\Delta t)$ as a function of the pendula natural periods for $\Delta t_w = 0.1$ s. Blue and red markers indicate the set used in (a) and the optimal set that minimizes Δt_{max}, respectively.

state $s = 0$ (Figure 1c). Thus, by precisely timing the actuation, we can deterministically set the pendulum to either state 0 or 1. Moreover, by raising the indenter, the pendulum is released into free oscillation, allowing the state to be reprogrammed by lowering the indenter again after a specific time window Δt (Figure 1c; Video S1). The pendulum retains the same state if $\Delta t \in \left[(n-1)T, (n-1)T + \frac{T}{4}\right] \cup \left[nT - \frac{T}{4}, nT\right]$, where T is the natural period of the pendulum and n is a positive integer. Conversely, it switches state if indentation occurs in $\Delta t \in \left[(n-1)T + \frac{T}{4}, nT - \frac{T}{4}\right]$. Finally, we emphasize that energy is required only to reposition the indenter. Once it is set in place, the indenter and the out-of-equilibrium pendula remain in a stable equilibrium configuration, as the holding ratchet of the servo motors is sufficient to maintain the state without any additional energy input.

3 | Collective Behavior of N Independent Hybrid Mechanical Bits

Next, we investigate the collective behavior of N independent hybrid mechanical bits subjected to simultaneous actuation by a vertically moving indenter. By assigning each pendulum a distinct natural period, we leverage their gradual desynchronization to access all 2^N possible system states. As an illustrative example, in Figure 2 we show results for an array of three pendula with periods $T_{\min} = 0.59$ s, $T_{\mathrm{mid}} = 0.61$ s, and $T_{\max} = 0.64$ s. At time $t = 0$, we initialize all pendula in state $s = 0$, placing the system in state $s_{\min}s_{\mathrm{mid}}s_{\max} = 000$. The pendula are then released to oscillate freely. To program a specific target state, we identify a time window Δt_{w} during which all three pendula simultaneously occupy the desired state. We note that the duration of the actuation window Δt_{w} must be shorter than half the smallest period in the array ($T_{\min}$), but large enough to ensure that the indenter can successfully lock each pendulum in place during it. In Figure 2a, the shaded regions mark the time intervals where the indenter must be lowered to reach all seven states from the initial 000 state when choosing $\Delta t_{\mathrm{w}} = 0.1$ s. Figure 2b presents the measured angular trajectories (Video S2), confirming that each pendulum can indeed be trapped in the desired state. For the chosen pendula and $\Delta t_{\mathrm{w}} = 0.1$ s, state 010 requires the longest time to be accessed, with $\Delta t = \Delta t_{\max} = 5.85\ \mathrm{s} \simeq 9.1 T_{\max}$.

The ability to efficiently program the system state enables reconfiguration of its mechanical response, which can be exploited for both functionality and state readout. As an example, we construct a reprogrammable linear spring by attaching elastomeric shells to the left side of each pendulum, such that indentation occurs only when the pendulum is in state $s = 1$. After programming a state, we apply an additional displacement u_{push} by further lowering the indenter, causing the pendula in state $s = 1$ to indent their shells while, we measure the resulting force–displacement response (see Section SII.B). The shells are fabricated by molding a VPS elastomer (Zhermack Elite Double 32) (see Section SI.B) and their mechanical response is tuned through the thickness-to-radius ratio d/R (Figure 2d; Figure S5). To ensure distinct responses, shells with $d/R = 0.2$, 0.3, and 1.0 (all with outer radius $R = 20$ mm) are placed on the left side of the pendula with periods $T_{\min}$, T_{mid}, and $T_{\max}$, respectively. Since each shell produces a different indentation response, each programmed state yields a distinct force–displacement curve (Figure 2e). This leads to two key outcomes. First, the system acts as a reprogrammable linear spring: selecting a particular bit configuration gives rise to a predictable, distinct mechanical response. Second, the one-to-one mapping between state and force–displacement curve provides

a robust state readout mechanism. Because these curves can be accurately reconstructed by summing the responses of the indented shells (dotted lines in Figure 2e), the underlying bit configuration can be identified by matching the measured response to this superposition (see Section SII.B), without requiring prior knowledge of the initial state or timing.

While the three pendula used in Figure 2a–e require up to 5.85 s to reach a system state starting from 000, this time can be substantially reduced by carefully selecting their natural periods. The maximum time interval Δt needed to access one of the seven system states from 000, denoted $\Delta t_{\max}$, cannot be shorter than $2^3\Delta t_w$. This lower bound is intuitively achieved by choosing $T_{\min} = 4\Delta t_w$, $T_{\mathrm{mid}} = 8\Delta t_w$, and $T_{\max} = 16\Delta t_w$ (see Section SIII.B and Figure S12 for details).

However, due to fabrication tolerances and spatial constraints, the pendulum periods in our experimental setup are restricted to the range $T \in [0.5, 0.8]$ s, making it impossible to realize the theoretical optimum. Instead, we systematically explore the allowable design space to identify the set of periods that minimizes $\Delta t_{\max}$ within these constraints. As shown by a red dot in Figure 2f, for $\Delta t_w = 0.1$ s, the optimal set within the permitted range corresponds to periods $T_{\min} = 0.63T_{\max} = 0.5$ s and $T_{\mathrm{mid}} = 0.78T_{\max} = 0.62$ s with the longest period set to $T_{\max} = 0.79$ s. With those three natural periods, all eight configurations are reached within $\Delta t_{\max} = 1.225\ \mathrm{s} \simeq 1.6T_{\max}$ when starting from state 000 (we recall the absolute possible minimum is $\Delta t_{\max} = 2^3\Delta t_w = 0.8$ s for $\Delta t_w = 0.1$ s).

The platform can be readily generalized to an arbitrary number of pendula and to transitions between any pair of system states. As a demonstration, we consider a system of five pendula, select five out of the 2^5 possible states, and search for the set of pendulum periods that minimizes the maximum transition time between any pair of the selected states. The chosen states are those in which only one pendulum is in state 1 and the others are in state 0 (namely, 10000, 01000, 00100, 00010, and 00001), yielding $N_s(N_s-1)/2 = 10$ unique state transitions, where N_s is the number of selected states (Figure 3a). Using the minimum achievable time window of our experimental setup, $\Delta t_w = 0.02$ s, we find the optimal set of pendulum periods to be $T = 0.50$, 0.54, 0.61, 0.67, 0.76 s. As shown in Figure 3a, for this configuration the shortest transition occurs between states 00010 and 00001 with $\Delta t = 0.44$ s, while the longest occurs between states 01000 and 00010 with $\Delta t = 2.375$ s. Because all transitions are completed within approximately three oscillation periods of the slowest pendulum, dissipative amplitude decay remains negligible over the programming interval.

4 | Robotic Hand

The five pendula can be viewed as the fingers of a robotic hand, each independently programmable to interact with external objects such as a keyboard or piano. To functionalize the system, we place a limit switch on the left side of each pendulum and connect it to an LED. After the pendula are programmed into a desired state (Figure 3b), an additional downward displacement u_{push} of about 2 mm is applied to the indenter, bringing any pendula that are in state $s = 1$ into contact with their switches and thereby activating the corresponding LEDs (Figure 3c). To reprogram the system while maintaining consistent oscillation amplitude, the indenter is displaced upward by about 2 mm before being released into free oscillation. This procedure ensures stability and repeatability across programming cycles.

By assigning a musical note to each sensor [24], the system can be programmed to play five-notes melodies, such as “Oh When the Saints” (Figure 3d), with the pendula acting as actuated ‘fingers’. In this demonstration, we map the notes Do, Re, Mi, Fa, and Sol to the states 00001, 00010, 00100, 01000, and 10000, respectively, and show that the platform can reproduce arbitrary songs composed of these five notes (Figure 3e; Figure S6 and S7, and Videos S3 and S4). The rhythm of the song is faithfully reproduced, with the musical tempo set by the longest Δt among the required state transitions, together with the motor control time (0.3 s) and the note-playing time (2 s). Here, $\Delta t = 2.375\ \mathrm{s} \simeq 3.1T_{\max}$ when playing Re followed by Fa, or vice versa. These factors yield a tempo of 4.7 s, as shown by the gray vertical lines separating consecutive notes in Figure 3d–e.

The system is not limited to the five states shown in Figure 3; it can be programmed to access all 2^5 states, corresponding to 496 possible transitions. These transitions, however, are not unique, since Δt depends only on which pendula flip and which remain unchanged. For example, the transition from 00100 to 01000 takes the same time as the transition from 01101 to 00001, as both involve flipping the second and third pendula while leaving the others unchanged (Figure 4a). We denote such transitions as $XFFXX$, where ‘F’ indicates a state flip and ‘X’ denotes no change. Consequently, although 496 transitions are possible, only 32 distinct Δt exist. This disparity indicates that the control signal provides only a scalar timing parameter, whereas the full N-bit information is encoded in the symmetry-broken orientations of the pendula. We therefore search for the pendulum periods that minimize the longest of these 32 transitions, Δt_{max}. We find that for $T = 0.50$, 0.53, 0.59, 0.65, and 0.78 s all 32 transitions occur in less than $3.225\ \mathrm{s} \simeq 4.1T_{\max}$ for $\Delta t_w = 0.02$ s (Figure 4a). As shown in Figure 4b, $\Delta t_{\max}$ depends strongly on the observation window Δt_w: larger Δt_w yields systematically longer $\Delta t_{\max}$, with the set of optimal natural periods also shifting. In the limit $\Delta t_w \to 0$, $\Delta t_{\max}$ approaches a plateau of 2.875 s. Notably, the experimentally employed window $\Delta t_w = 0.02$ s already lies in a regime where all states are accessible within a few oscillation periods, corresponding to a timing resolution that is small compared to the natural periods of the pendula. As a result, dissipation remains weak over the programming interval and oscillation amplitudes remain sufficiently large, reducing susceptibility to small perturbations in the reset height.

Accessing any state within a bounded actuation time enables the system to play arbitrary sequences of notes and chords. To demonstrate this, we fabricated the set of pendula that minimizes $\Delta t_{\max}$ across all 32 possible transitions and programmed the system to reproduce a 12-chords progression from the chorus of “Smoke on the Water” (Figure 4c). In this demonstration, the notes Do, Re, Mi, Sol, and La are mapped to the states 00001, 00010, 00100, 10000, and 01000, respectively, with chords formed by simultaneously activating multiple notes. For instance, the first three chords of the progression are realized by programming the system into states 01100, 10001, and 01010 (Figure 4d;

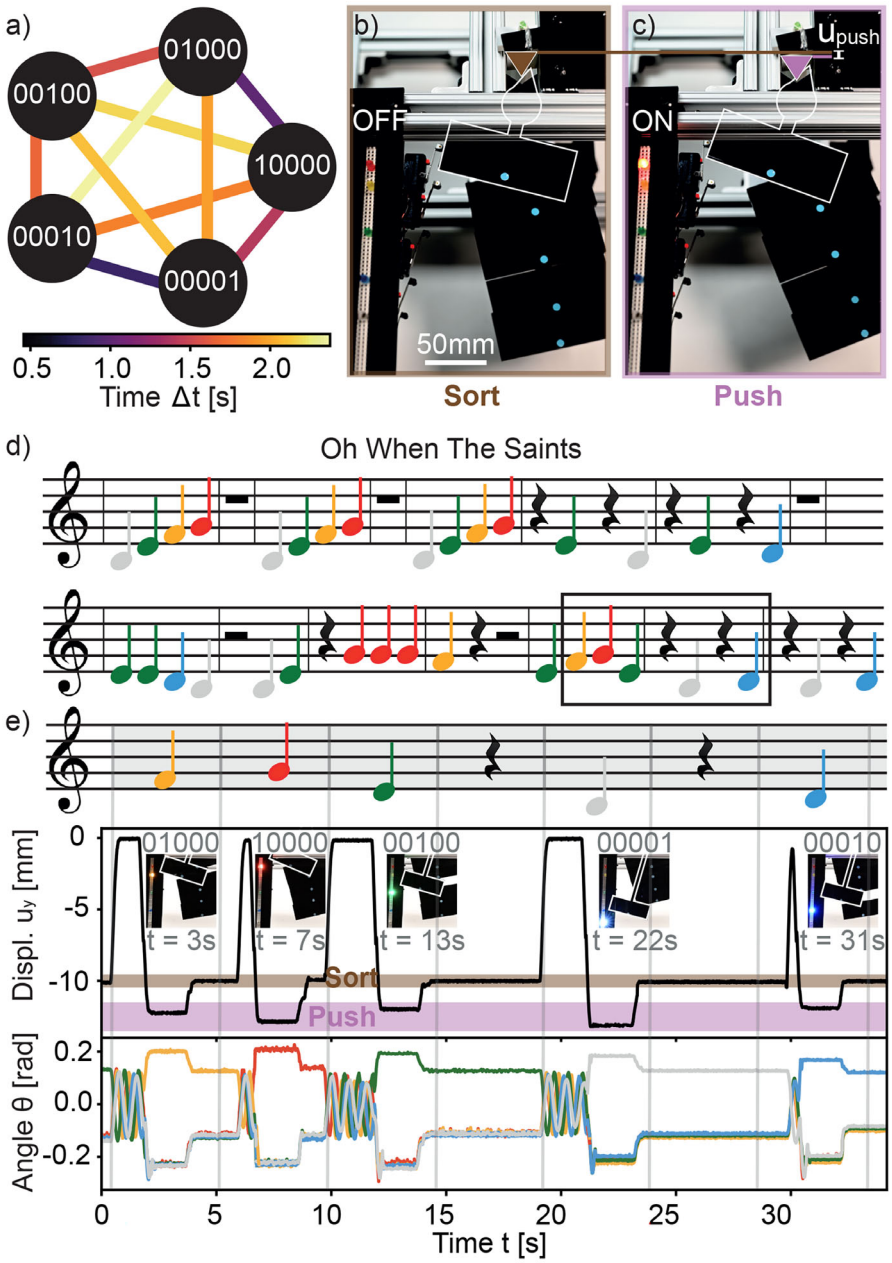

FIGURE 3 | Playing five-notes songs. (a) Diagram of all possible transitions between the five states, with colored arrows indicating the transition times Δt. (b) The system sorted into state 10000 by lowering the indenter. (c) A further 2 mm downward displacement of the indenter brings the pendulum in state $s = 1$ into contact with its switch, switching on the red LED. (d) Chorus of "Oh When the Saints" (34-notes sequence). (e) Experimental demonstration of a five-note sequence from "Oh When the Saints". Top: notes and rest times; middle: indenter displacement over time with snapshots showing the pendula activating the corresponding LEDs; bottom: pendulum angles θ over time.

Figure S8, and Video S5). The rhythm of the song is faithfully captured by adjusting the resting times between transitions in proportion to the pendula sorting time, ensuring a musical tempo of 4.2 s (the longest transition used in the song is *FFXFF* with $\Delta t = 1.9$ s).

5 | Conclusion

In summary, we have demonstrated that arrays of oscillating pendula, with symmetry broken by kinematic boundary conditions, can be programmed to function as mechanical bits. The system state is dictated solely by the timing of a global actuation signal, which can be tuned to access desired configurations. Importantly, the required timing precision remains moderate, as demonstrated by our simple macroscale experimental implementation. This platform enables reprogrammable mechanical responses, arbitrary information encoding, and the implementation of a mechanical piano capable of executing user-defined note sequences within only a few oscillation periods of the slowest pendulum.

Beyond the specific realization presented here, our results highlight a general strategy for mechanical reprogrammability: the use

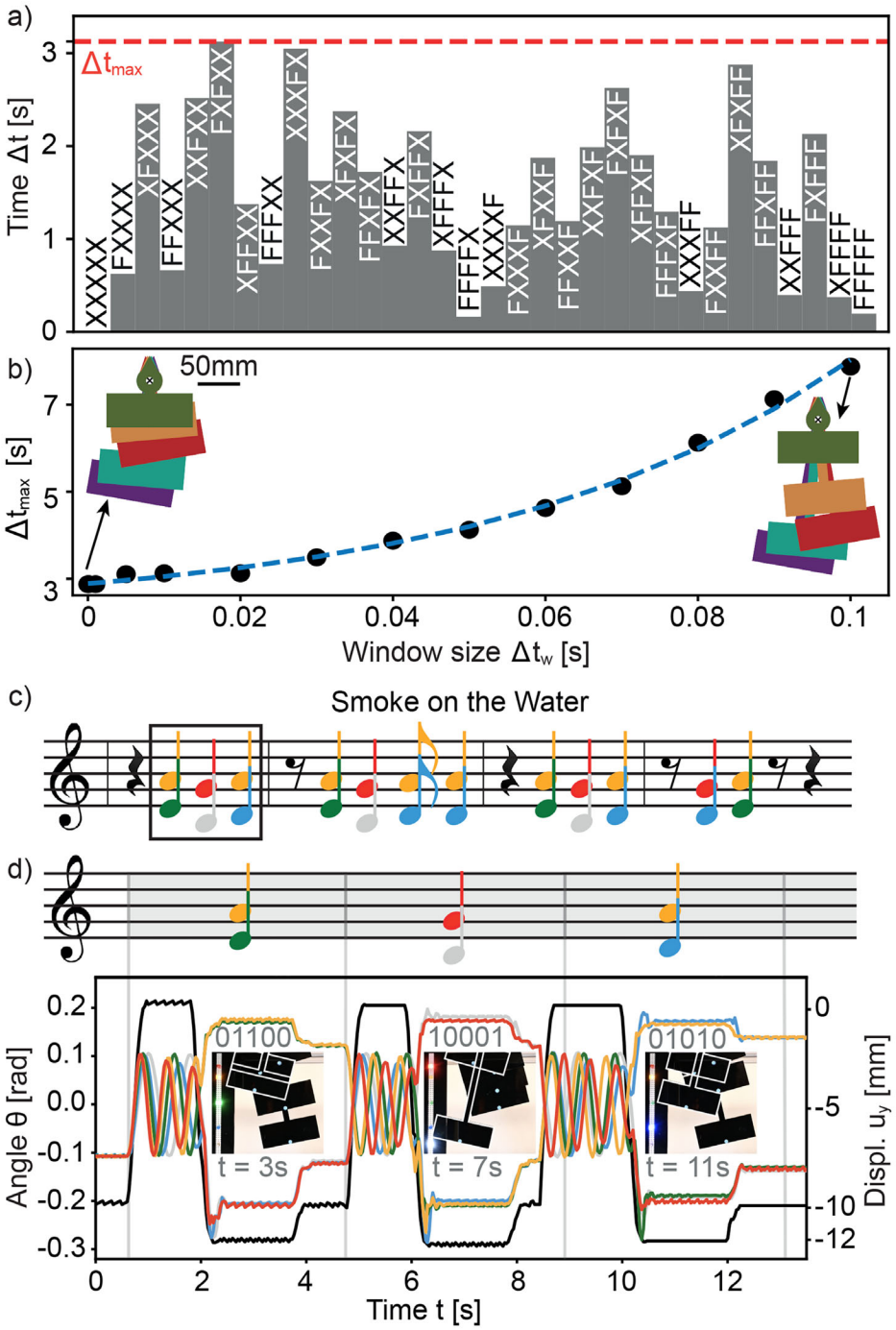

FIGURE 4 | Accessing all 32 states. (a) Transition times Δt for the 32 distinct state changes, using pendulum periods chosen to minimize the maximum transition time Δt_{max}. (b) Dependence of Δt_{max} on the observation window Δt_w. (c) Chorus of "Smoke on the Water" (12-chords sequence). (d) Experimental demonstration of a three-chords sequence from "Smoke on the Water". Right axis: indenter displacement over time (black lines). Left axis: pendulum angles θ over time (colored lines). Insets: snapshots from Video S5.

of a single global temporal control parameter to access an exponentially large discrete state space. In our system, continuous phase evolution (an analog process) is translated into deterministic digital state selection through controlled desynchronization and symmetry breaking. This hybrid analog–digital architecture enables multiple configurations to be addressed without spatially encoding information in the actuation signal, thereby providing a scalable pathway toward globally programmable dynamical systems.

By integrating multiple functionalities within a single framework, our approach establishes a new class of scalable systems that exploit dynamics for simple and efficient mechanical reprogramming. Although our experiments employed pendula as mechanical bits, the underlying mechanism of frequency separation combined with global boundary modulation and phase-dependent state selection readily generalizes to other oscillatory systems. The essential ingredients are desynchronized oscillatory elements, a global control parameter, and a mechanism to

transiently constrain and release their motion – features that are widely available across mechanical, fluidic, and electronic oscillator networks. In particular, elastic oscillators like membranes or beams [25], which are now relatively easy to make at the microscopic scale [26], could provide faster and more scalable reprogrammability. More broadly, the same principles may inspire analogous platforms in fluids [27], chemical oscillators [28], and electronic circuits [29], all of which inherently exhibit oscillations and multistability, underscoring the universality of dynamics as a pathway to reprogrammable matter.

Acknowledgements

K.B. acknowledges support from the Simons Collaboration on Extreme Wave Phenomena Based on Symmetries. G.R. acknowledges support from the Swiss National Science Foundation under Grant No. P500PT-217901. A.L acknowledges support from the French National Center for Scientific Research for hosting him in a CNRS delegation.

Data Availability Statement

The data supporting the experimental results in this study are available from the corresponding author upon request.

Conflicts of Interest

The authors declare no conflicts of interest.

References

1. Y. Kim, H. Yuk, R. Zhao, S. A. Chester, and X. Zhao, "Printing Ferromagnetic Domains for Untethered Fast-Transforming Soft Materials," *Nature* 558, no. 7709 (2018): 274–279.

2. S. Wu, Q. Ze, J. Dai, N. Udipi, G. H. Paulino, and R. Zhao, "Stretchable Origami Robotic Arm with Omnidirectional Bending and Twisting," *Proceedings of the National Academy of Sciences* 118, no. 36 (2021): e2110023118, https://www.pnas.org/doi/10.1073/pnas.2110023118.

3. A. S. Gladman, E. A. Matsumoto, R. G. Nuzzo, L. Mahadevan, and J. A. Lewis, "Biomimetic 4D Printing," *Nature Materials* 15 (2016): 413–418, https://doi.org/10.1038/nmat4544.

4. E. Brown, N. Rodenberg, J. Amend, et al., "Universal Robotic Gripper Based on the Jamming of Granular Material," *Proceedings of the National Academy of Sciences* 107, no. 44 (2010): 18809–18814.

5. Y. Wang, B. Ramirez, K. Carpenter, C. Naify, D. C. Hofmann, and C. Daraio, "Architected Lattices with Adaptive Energy Absorption," *Extreme Mechanics Letters* 33 (November 2019): 100557.

6. J. D. Brigido-González, S. G. Burrow, and B. K. S. Woods, "Switchable Stiffness Morphing Aerostructures Based on Granular Jamming," *Journal of Intelligent Material Systems and Structures* 30, no. 17 (October 2019): 2581–2594.

7. P. Wang, F. Casadei, S. Shan, J. C. Weaver, and K. Bertoldi, "Harnessing Buckling to Design Tunable Locally Resonant Acoustic Metamaterials," *Physical Review Letters* 113, no. 1 (2014): 014301.

8. B. Florijn, C. Coulais, and M. van Hecke, "Programmable Mechanical Metamaterials," *Physical Review Letters* 113 (October 2014): 175503, https://link.aps.org/doi/10.1103/PhysRevLett.113.175503.

9. P. M. Reis, "A Perspective on the Revival of Structural (In)Stability with Novel Opportunities for Function: From Buckliphobia to Buckliphilia," *Journal of Applied Mechanics* 82, no. 11 (November 2015): 111001.

10. C. Coulais, E. Teomy, K. de Reus, Y. Shokef, and M. van Hecke, "Combinatorial Design of Textured Mechanical Metamaterials," *Nature* 535, no. 7613 (2016): 529–532, https://doi.org/10.1038/nature18960.

11. J. A. Faber, J. P. Udani, K. S. Riley, A. R. Studart, and A. F. Arrieta, "Dome-Patterned Metamaterial Sheets," *Advanced Science* 7, no. 22 (2020): 2001955.

12. H. Yasuda, P. R. Buskohl, A. Gillman, et al., "Mechanical Computing," *Nature* 598, no. 7879 (2021): 39–48.

13. B. Treml, A. Gillman, P. Buskohl, and R. Vaia, "Origami Mechanologic," *Proceedings of the National Academy of Sciences* 115, no. 27 (2018): 6916–6921.

14. T. Chen, M. Pauly, and P. M. Reis, "A Reprogrammable Mechanical Metamaterial with Stable Memory," *Nature* 589, no. 7842 (2021): 386–390.

15. B. Gorissen, D. Reynaerts, S. Konishi, K. Yoshida, J. W. Kim, and M. De Volder, "Elastic Inflatable Actuators for Soft Robotic Applications," *Advanced Materials* 29, no. 43 (2017): 1604977.

16. L. J. Kwakernaak and M. van Hecke, "Counting and Sequential Information Processing in Mechanical Metamaterials," *Physical Review Letters* 130, no. 26 (June 2023): 268204.

17. J. Liu, M. Teunisse, G. Korovin, et al., "Controlled Pathways and Sequential Information Processing in Serially Coupled Mechanical Hysterons," *Proceedings of the National Academy of Sciences* 121, no. 22 (2024): e2308414121, https://www.pnas.org/doi/abs/10.1073/pnas.2308414121.

18. E. Gutierrez-Prieto, C. M. Meulblok, M. van Hecke, and P. M. Reis, "Dynamic Driving Enables Independent Control of Material Bits for Targeted Memory," 2025, https://arxiv.org/abs/2508.16257.

19. A. Lazarus, "Discrete Dynamical Stabilization of a Naturally Diverging Mass in a Harmonically Time-Varying Potential," *Physica D: Nonlinear Phenomena* 386 (2019): 1–7.

20. A. A. Grandi, S. Protière, and A. Lazarus, "Enhancing and Controlling Parametric Instabilities in Mechanical Systems," *Extreme Mechanics Letters* 43 (2021): 101195.

21. A. A. Grandi, S. Protière, and A. Lazarus, "New Physical Insights in Dynamical Stabilization: Introducing Periodically Oscillating-Diverging Systems (Pods)," *Nonlinear Dynamics* 111, no. 13 (2023): 12339–12357.

22. I. Mahboob and H. Yamaguchi, "Bit Storage and Bit Flip Operations in an Electromechanical Oscillator," *Nature Nanotechnology* 3, no. 5 (2008): 275–279.

23. Z. P. Bažant and L. Cedolin, *Stability of Structures: Elastic, Inelastic, Fracture and Damage Theories* (World Scientific, 2010).

24. B. Van Raemdonck, E. Milana, M. De Volder, D. Reynaerts, and B. Gorissen, "Nonlinear Inflatable Actuators for Distributed Control in Soft Robots," *Advanced Materials* 35, no. 35 (2023): 2301487.

25. R. D. Blevins, *Formulas for Dynamics, Acoustics and Vibration* (John Wiley & Sons, 2015).

26. G. Pillai and S. S. Li, "Piezoelectric MEMS Resonators: A Review," *IEEE Sensors Journal* 21, no. 11 (2020): 12589–12605.

27. M. C. Cross and P. C. Hohenberg, "Pattern Formation Outside of Equilibrium," *Reviews of Modern Physics* 65 (July 1993): 851–1112, https://link.aps.org/doi/10.1103/RevModPhys.65.851.

28. I. Epstein and J. Pojman, *An Introduction to Nonlinear Chemical Dynamics: Oscillations, Waves, Patterns, and Chaos*, ser. Topics in Physical Chemistry (Oxford University Press, 1998), https://books.google.it/books?id=ci4MNrwSlo4C.

29. S. H. Strogatz, *Chemistry Applications to Physics, Biology, and Engineering, Nonlinear Dynamics and Chaos* (Addison-Wesley, 1994).

Supporting Information

Additional supporting information can be found online in the Supporting Information section.

Supporting File 1: adfm75229-sup-0001-SuppMat.pdf.

Supporting File 2: adfm75229-sup-0002-SupVideo1.mp4.

Supporting File 3: adfm75229-sup-0003-SupVideo2.mp4.

Supporting File 4: adfm75229-sup-0004-SupVideo3.mp4.
Supporting File 5: adfm75229-sup-0005-SupVideo4.mp4.
Supporting File 6: adfm75229-sup-0006-SupVideo5.mp4.